CHEMISTRY
A EUROPEAN JOURNAL

DOI: 10.1002/chem.200700237

Intramolecular Mixed-Valence State Through Silicon or Germanium Double Bridges in Rigid Bis(Tetrathiafulvalenes)

Frédéric Biaso,[a] Michel Geoffroy,*[a] Enric Canadell,[b] Pascale Auban-Senzier,[c] Eric Levillain,[d] Marc Fourmigué,[d] and Narcis Avarvari*[d]

Abstract: The synthesis and characterization of two *ortho*-dimethyltetrathiafulvalene (*o*-DMTTF)-based rigid dimers containing dimethylsilicon (Me_2Si) or dimethylgermanium (Me_2Ge) linkers are described. Single-crystal X-ray analysis reveals planar geometry for the central 1,4-disilicon or 1,4-digermanium six-membered rings. DFT calculations provide optimized conformations in agreement with the experimental ones, and also emphasize the role of the heteroatomic linkers in the conjugation between the two redox active units. Cyclic voltammetry measurements show sequential oxidation into radical cation, and then dication species. Solution EPR measurements on the radical-cation species indicate full delocalization of the unpaired electron over both electroactive TTF units, with an associated coupling of 0.42 G with twelve equivalent protons. DFT calculations afford fully planar geometry for the radical-cation species and confirm the experimental isotropic coupling constant. Single-crystal X-ray analyses of two charge-transfer compounds obtained upon chemical oxidation, formulated as $[(Me_2Si)_2(o\text{-}DMTTF)_2]\cdot 1/2[TCNQ]\cdot 1/2[TCNQF_4]$ and $[(Me_2Ge)_2(o\text{-}DMTTF)_2]\cdot[TCNQ]$, demonstrate the occurrence of genuine mixed-valence radical-cation species, as well as a three-dimensional network of short S···S intermolecular contacts. Temperature-dependent conductivity measurements demonstrate semiconducting behavior for both charge-transfer compounds, with an increase of the absolute value of the conductivity upon applying external pressure. Band structure calculations reveal peculiar pseudo-two-dimensional electronic structures, also confirming electronic interactions through $SiMe_2$ and $GeMe_2$ bridges.

Keywords: conducting materials · EPR spectroscopy · main group elements · mixed-valent compounds · tetrathiafulvalenes

Introduction

The access to intramolecular mixed-valence states in a perfectly controlled manner is one of the main purposes of the efforts devoted to the synthesis of dimeric tetrathiafulvalenes (TTF),[1] because TTFs represent a class of precursors extensively studied in the quest for molecular conductors and superconductors.[2] In such multiredox compounds, the degree of electronic communication between the redox-active units is governed by the magnitude of through-bond or through-space interactions, accounting for the occurrence and, ultimately, isolation, either in solution or solid state, of mixed-valence species. As a consequence, charge-transfer (CT) complexes or radical-cation salts derived from dimeric TTFs might exhibit unusual structures due to the enhancement of the dimensionality, with peculiar band-structure patterns and band fillings.[3] A straightforward strategy to link two TTF units in close vicinity relies on the utilization of heteroatom bridges, such as within the series of $X(TTF)_2$-type derivatives (X = S,[4] Se,[4] Te,[5] PPh,[6] $SiMe_2$,[6a] Hg[6a]).

[a] Dr. F. Biaso, Prof. M. Geoffroy
Department of Physical Chemistry, University of Geneva
30 Quai Ernest Ansermet, 1211 Geneva (Switzerland)
Fax: (+41) 22-379-6103
E-mail: Michel.Geoffroy@chiphy.unige.ch

[b] Dr. E. Canadell
Institut de Ciència de Materials de Barcelona (CSIC)
Campus de la UAB, 08193 Bellaterra (Spain)

[c] Dr. P. Auban-Senzier
Laboratoire de Physique des Solides, UMR 8502
Bât. 510, Université Paris-Sud, 91405 Orsay (France)

[d] Dr. E. Levillain, Dr. M. Fourmigué, Dr. N. Avarvari
Laboratoire Chimie, Ingénierie Moléculaire et Matériaux (CIMMA)
UMR 6200 CNRS-Université d'Angers, UFR Sciences
Bât. K, 2 Bd. Lavoisier, 49045 Angers (France)
Fax: (+33) 02-4173-5405
E-mail: narcis.avarvari@univ-angers.fr

Supporting information for this article is available on the WWW under http://www.chemeurj.org/ or from the author.

Yet, single-crystal X-ray analyses of some of these compounds show that in the solid state the two TTF units are not coplanar, but are organized in a nearly perpendicular manner with respect to each other, thus completely hampering the possibility of extended conjugation.[4–7] In this respect, molecular rigidity has been achieved upon introduction of a second heteroatom bridge, within donors formulated as $X_2(TTF)_2$ in which two TTF units are linked either by two sulfur (X=S)[8] or tellurium (X=Te)[9] atoms, or, as described more recently, by two phenylphosphino groups (X=PPh),[10] thus leading to the formation of a central six membered ring.

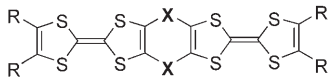

Alternatively, two tetraselenafulvalene (TSF) units have been connected through methylantimony groups to provide $(MeSb)_2(TSF)_2$.[11] Nevertheless, within all the heteroatom containing rigid dimeric bis(TTF) described so far, no clear evidence, such as EPR measurements, for the electron delocalization throughout both TTF units in the radical-cation species has been provided. Highly appealing heteroatom-based bridges consist of dialkylsilicon or dialkylgermanium linkers. Indeed, the former has been successfully employed in the synthesis of rigid, doubly bridged metallocenes with multiple redox states.[12] Moreover, the use of R_2Si or R_2Ge bridges would avoid the formation of *cis/trans* isomers encountered in the case of $(PPh)_2(o\text{-DMTTF})_2$[10] or $(MeSb)_2(TSF)_2$.[11] We report herein the synthesis of unprecedented rigid dimeric TTFs formulated as $(Me_2Si)_2(o\text{-DMTTF})_2$ and $(Me_2Ge)_2(o\text{-DMTTF})_2$. The latter also represents the first germanium-containing TTF derivative. We also report on solution EPR measurements of the intramolecular mixed-valence radical-cation species of both compounds, correlated with theoretical calculations, as well as on the preparation and properties of two crystalline conducting CT compounds of these new donors.

Results and Discussion

The synthesis of $(Me_2E)_2(o\text{-DMTTF})_2$, E=Si (**1**) and Ge (**2**), is straightforward; that is, bis-lithiation of the *ortho*-dimethyltetrathiafulvalene (*o*-DMTTF) precursor followed by trapping the dianionic intermediate with Me_2ECl_2 in a one-pot procedure (Scheme 1).[13] The new donors were obtained as orange-yellow crystalline solids and were fully characterized.

Suitable single-crystals for X-ray analysis were successfully grown for both compounds. Even though they are not isostructural, their molecular conformation with respect to the planarity of the central six-membered ring is essentially the same; therefore, we discuss hereafter only the structure of the silicon compound **1**.

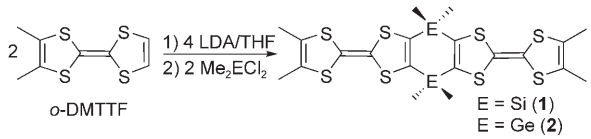

Scheme 1. Synthesis of $(Me_2Si)_2(o\text{-DMTTF})_2$ (**1**) and $(Me_2Ge)_2(o\text{-DMTTF})_2$ (**2**).

The most striking structural feature lies clearly in the full planarity of the central silicon-containing six-membered ring (Figure 1). This is in sharp contrast to the structures of Te-[9]

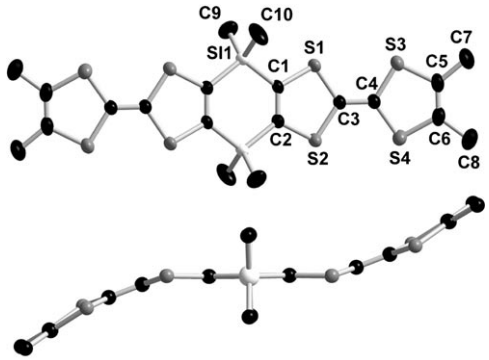

Figure 1. ORTEP view of **1** (thermal ellipsoids set at 50% probability, H atoms omitted) (top) and side view of the molecule (bottom). Selected bond lengths [Å] and angles [°]: Si1–C1 1.870(3), Si1–C2* 1.869(3), C1–C2* 1.347(3), C3–C4 1.343(4), C1-Si1-C2 107.1(1). Folding angles [°]: Si1···Si1* 0.0(1), S1···S2* 20.0(2), S3···S4 11.7(3). Symmetry operator for generating equivalent atoms (*): $-x$, $1-y$, $-z$.

or P-[10] containing rigid TTF dimers, for which folding angles of 67.8° and 30.4°, respectively, for the central ring have been observed. Note also that various folding angles along the Si···Si hinge, leading to boat conformations, have been reported in the case of doubly silicon-bridged metallocenes.[12c,e,14] The overall geometry of **1** is bent within a chair-like conformation, mainly due to the folding along the S1···S2 hinges amounting to 20°. Bond lengths and angles are typical for a neutral TTF derivative, with the central C3–C4 double bond at 1.343(4) Å and the average of the central C–S bonds at 1.753 Å. The planarity of the central ring might suggest some conjugation between the TTF moieties through the $SiMe_2$ bridges, as pointed out within a series of bis(silicon)-bridged stilbene homologues, for which an orbital interaction between the Me_2Si σ* orbital and the stilbene π* orbital has been evidenced, leading to a stabilization of the LUMO.[15] The same features are also present in the structure of the germanium compound **2** (Supporting Information). In order to estimate the extent of the communication between the symmetrical TTF units and to evidence the role of the $SiMe_2$ and $GeMe_2$ bridges, we performed theoretical calculations at the DFT level.[13] The optimized geometries are in good agreement with the experimental structures, reproducing the planarity of the central six-membered ring and the chair conformation of the molecule (Figure 2).

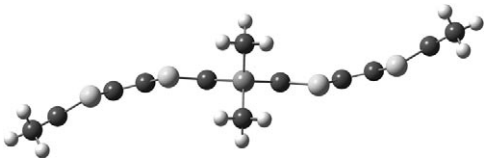

Figure 2. Optimized geometry of **1**.

The analysis of the generated frontier orbitals is particularly interesting. First, an increase in degeneracy is observed at the HOMO level, thus providing a pair of π-type HOMOs, as an antisymmetric combination, and HOMO−1, as an symmetric combination, with an energy gap of 82 meV, indicative of a sizeable electronic communication between the TTF units. Secondly, the composition of the LUMO clearly evidences the role of the $SiMe_2$ bridge in the conjugation, as we observe favorable orbital overlaps between the $SiMe_2$ σ* orbitals and the vinylic π* orbitals (Figure 3).

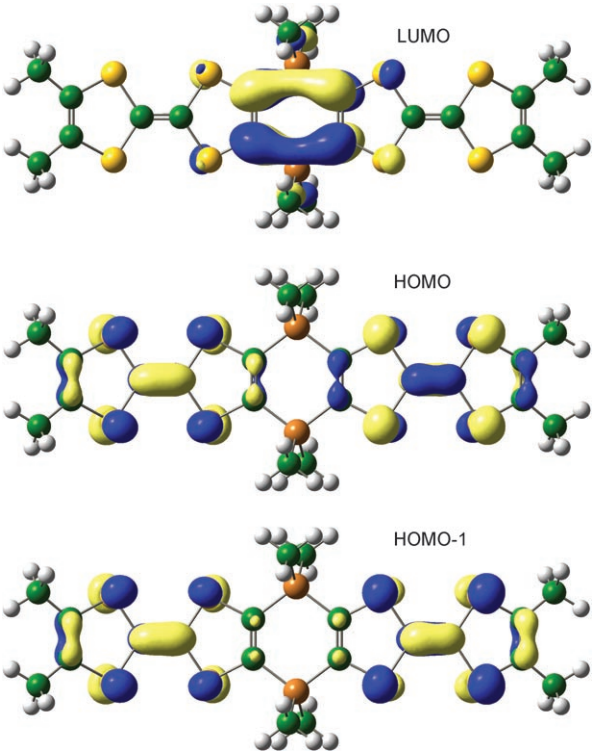

Figure 3. HOMO−1 (bottom), HOMO (middle) and LUMO (top) of optimized **1**.

Analogous results are obtained in the case of the germanium compound **2**,[13] with a HOMO/HOMO−1 gap of 60 meV and the HOMO level at −4.631 eV, suggesting an increased electron-donating character relative to the silicon compound **1** (HOMO at −4.653 eV). Cyclic voltammetry measurements on both donors show sequential reversible oxidations to radical cations ($\mathbf{1}^{\bullet+}$ and $\mathbf{2}^{\bullet+}$) and then to the corresponding dication species, with associated potential differences in between of 120 mV for **1** and 110 mV for **2**

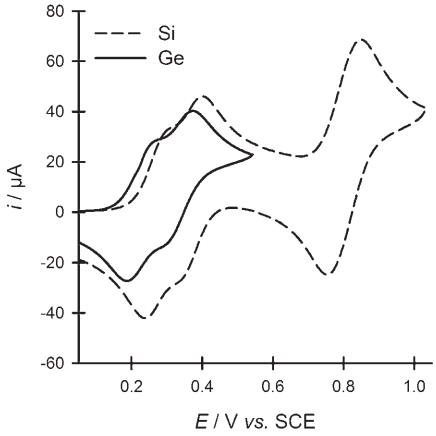

Figure 4. Cyclic voltammogram of **1** (Si) and **2** (Ge); potential values (V vs. SCE): $E_1=0.255$ ($\mathbf{1}^{\bullet+}$), $E_2=0.375$ ($\mathbf{1}^{2+}$), $E_3=0.79$ V ($\mathbf{1}^{4+}$); $E_1=0.225$ ($\mathbf{2}^{\bullet+}$), $E_2=0.335$ V ($\mathbf{2}^{2+}$).

(Figure 4), thus demonstrating sizeable electronic communication between the TTF units. Note the more facile oxidation of the germanium compound ($E_1=0.225$ V) relative to that of silicon ($E_1=0.255$ V).

It is thus clear that the selective generation of the mixed-valence radical-cation species from both donors, upon one-electron oxidation, should be feasible either electrochemically, or by chemical oxidation. This prompted us to undertake a solution EPR study in order to emphasize the formation of the corresponding radical cations and, more importantly, to have an ultimate proof about the electron delocalization within the molecule. Both compounds were thus oxidized in CH_2Cl_2 by one equivalent of $NOSbF_6$ and their EPR spectra recorded.

The hyperfine structure observed after oxidation of $(Me_2Si)_2$(*o*-DMTTF)$_2$ (Figure 5) is clearly consistent with the central part of a spectrum exhibiting a coupling of 0.42 G with 12 magnetically equivalent protons.[16] Moreover, a single hyperfine coupling constant ($A_{iso}=1.2$ MHz) is

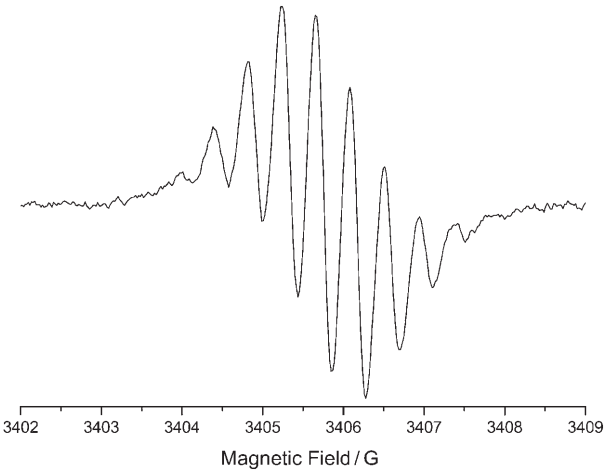

Figure 5. EPR spectrum of $\mathbf{1}^{\bullet+}$ (CH_2Cl_2, 1 equiv $NOSbF_6$, $\nu=9572$ MHz, $T=300$ K); $g_{iso}=2.0081$, $A_{iso}=0.42$ G.

detected on the ^{1}H ENDOR spectrum.[13] The hyperfine structure is thus due to the coupling with four methyl groups, the corresponding constant amounting to half the value previously measured on a mono-TTF derivative containing two Me groups in lateral positions.[17] This clearly demonstrates that in $\mathbf{1}^{\bullet+}$ the unpaired electron is delocalized over both TTF units. Note that the same EPR spectrum is observed when the oxidation is carried out electrochemically at the appropriate potential value, in situ in the EPR cavity with an electrolytic cell allowing us to work at a controlled potential. The same EPR spectra were obtained with $(Me_2Ge)_2(o\text{-DMTTF})_2$.[13] To rationalize the EPR results, we performed unrestricted DFT calculations on the radical-cation species of **1** and **2**.[13] In both cases the optimized geometry is fully planar and the singly occupied molecular orbital (SOMO), consisting of the antisymmetrical combination of TTF π orbitals, is delocalized on the two redox active units with a negligible contribution of Si or Ge atoms (Figure 6 for $\mathbf{1}^{\bullet+}$, see Supporting Information for $\mathbf{2}^{\bullet+}$).

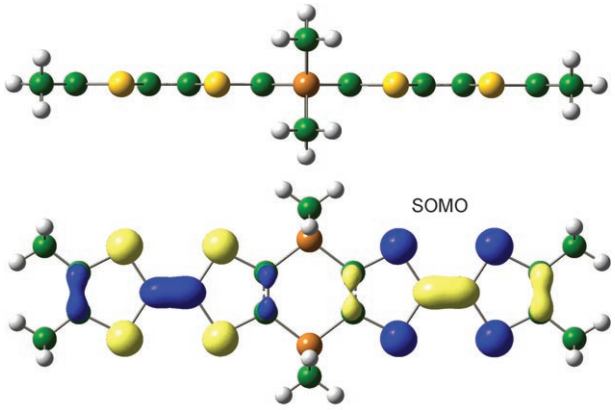

Figure 6. Optimized geometry of $\mathbf{1}^{\bullet+}$ (top) and SOMO (bottom).

Also, the calculated isotropic hyperfine coupling constant with the lateral methyl protons amounts to 0.49 G, in good agreement with the experimental value of 0.42 G (vide supra), while the coupling with the $SiMe_2$ protons is much weaker (−0.04 G), and thus, not surprisingly, it was not observed in the experimental EPR spectrum. With respect to the experimental and theoretical evidences, the new donors **1** and **2** can be regarded as Class III compounds if one refers to the Robin and Day classification of the mixed-valence systems, with strong coupling between the electroactive units, despite the saturated EMe_2 bridges.[18] These results prompted us to attempt the preparation of mixed-valence salts derived from **1** and **2** in the solid state. Our rigid dimers indeed afforded, upon simple chemical oxidation with one equivalent of a 1:1 TCNQ (tetracyanoquinodimethane)/$TCNQF_4$ (tetrafluoro-tetracyanoquinodimethane) mixture in the case of **1** or only TCNQ in the case of **2**, and subsequent slow evaporation of solvent, single crystals of two isostructural CT compounds formulated as **[1]**•1/2[TCNQ]•1/2[$TCNQF_4$] and **[2]**•[TCNQ], respectively.[13] The better electron-donating properties of **2** relative to **1** very likely allowed its oxidation by the TCNQ acceptor in solution, whereas $TCNQF_4$ was required to promote the oxidation of **1**, then both acceptors co-crystallized in a 1:1 ratio in their reduced form with the radical cation of the donor. The two isostructural mixed-valence CT compounds crystallize in the monoclinic system, space group *C*2/*m*, with the molecules of donors located in a special position, consisting of a mirror plane on the long axis of the molecule and a C_2 axis along the E···E hinge (E = Si, Ge), while the acceptor molecules are contained in a mirror plane and a C_2 axis passes through the middle of the central C=C double bonds. We detail hereafter only the structure of the mixed-valence salt of **1**.[13]

The donor molecule is now completely planar (Figure 7), thus confirming the results of the theoretical calculations. Moreover, the bond lengths values are in good agreement

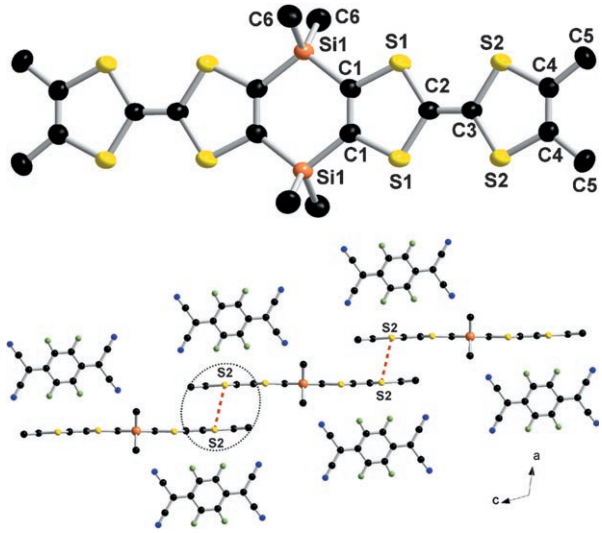

Figure 7. ORTEP view of $\mathbf{1}^{\bullet+}$ in the CT compound **[1]**•1/2[TCNQ]•1/2-[$TCNQF_4$] (thermal ellipsoids set at 50% probability, H atoms omitted) (top). Chains of donors and acceptors along *c* (bottom); the red dashed line S2···S2 characterizes the interaction I, whereas the dotted ellipse highlights an intermolecular $(TTF_2)^{\bullet+}$ fragment. Selected bond lengths [Å]: Si1−C1 1.878(4), C1−C1* 1.357(8), C2−C3 1.373(8). Intermolecular distances [Å]: S2···S2$^{\#}$ 3.726. Symmetry operator for generating equivalent atoms: (*) $x, -y, z$; ($^{\#}$) $1-x, y, 1-z$.

with those for a mixed-valence species.[2] Indeed, the central C2−C3 double bond lengthens to 1.373(8) Å, to be compared with 1.343(4) Å in neutral **1**, while the average of the central C−S bonds decreases now to 1.737 Å (1.753 Å in neutral **1**). These geometrical characteristics for $\mathbf{1}^{\bullet+}$, but also $\mathbf{2}^{\bullet+}$, combined with the analysis of the geometrical parameters of TCNQ,[19] indicating a donor–acceptor charge transfer of 1, strongly support the assumption of mixed-valence charge-transfer compounds with a mean charge of +0.5 on each TTF unit. The donors are longitudinally shifted along the *c* axis and interact along the *a* axis in the *ac* plane, through a favorable axial overlap (interaction I) between the external dithiol moieties, which is characterized by an

intermolecular S2···S2 contact at 3.726 Å, comparable with the sum of the van der Waals radii (3.70 Å) of two S atoms (Figure 7).[20] Furthermore, additional S2···S2 intermolecular contacts at 4.030 Å (interaction II; Figure 8) are established in the *ab* plane, thus leading to the formation of a two-dimensional array containing channels in which acceptor molecules reside. These molecules are isolated with respect to each other and disposed perpendicularly to the donors and to the *b* axis, an original feature within this type of compounds (Figure 8).[8b]

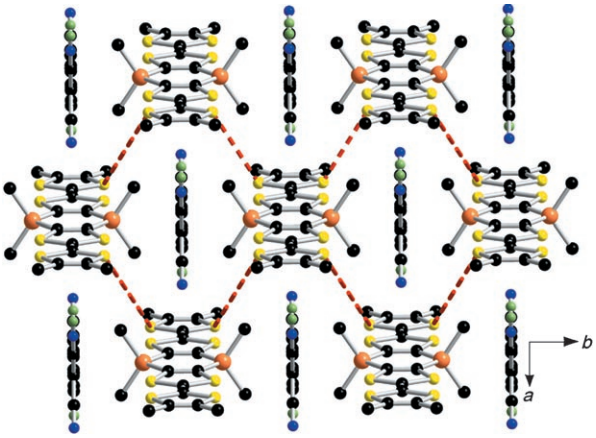

Figure 8. Packing diagram of the CT compound [**1**]·1/2[TCNQ]·1/2-[$TCNQF_4$] in the *ab* plane with an emphasis on the short intermolecular S2···S2 (0.5−*x*, 0.5−*y*, 1−*z*) distance of 4.030 Å (red dash line), characterizing the interaction II.

Four-probe single-crystal conductivity measurements were successfully performed on both CT compounds and they are indicative of semiconducting behavior, with room temperature conductivities of $6\times10^{-2}\,S\,cm^{-1}$ for the Si compound and $3\times10^{-3}\,S\,cm^{-1}$ for the Ge one, a value which strongly increases up to $0.2\,S\,cm^{-1}$ under applied pressure of 22 kbar in the case of the latter (Figure 9).[13]

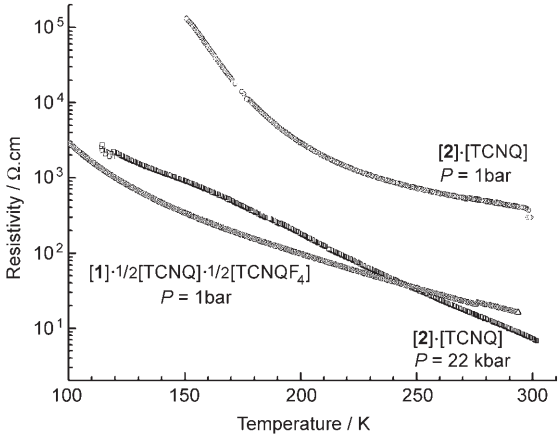

Figure 9. Single-crystal resistivity measurements for [**1**]·1/2[TCNQ]·1/2-[$TCNQF_4$] and [**2**]·[TCNQ].

Interesting insight was afforded by band structure calculations (Figure 10).[13]

With the charge +1 per donor molecule, the upper band should be empty, and, moreover, because of the symmetry

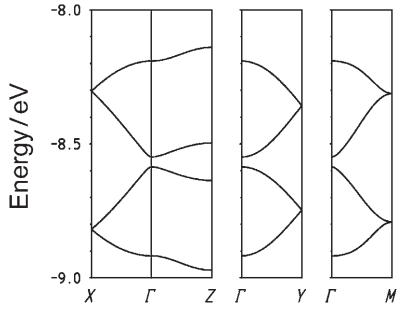

Figure 10. Band structure for [**1**]·1/2[TCNQ]·1/2[$TCNQF_4$]. $\Gamma=(0, 0, 0)$, $X=(a^*/2, 0, 0)$, $Y=(0, b^*/2, 0)$, $Z=(0, 0, c^*/2)$, and $M=(a^*/2, b^*/2, c^*/2)$.

of the structure, the bands necessarily touch in the points *X*, *Y*, and *M*, thus avoiding the establishment of an energy gap at the Fermi level. Therefore, the semiconducting behavior must result from electron localization due to electron repulsions. Essentially, our system can be described as a series of intermolecular $(TTF_2)^{\bullet+}$ fragments (as highlighted in Figure 7, interaction I) that communicate through either the EMe_2 bridges or the S···S contact of interaction II. Calculation of the Fermi surface of the system assuming a metallic filling of the bands[13] shows that, if the metallic state can be stabilized, our compounds should be pseudo-two-dimensional metals without any possibility for a Peierls transition to occur.

Conclusion

Original rigid TTF-based dimers containing $SiMe_2$ and $GeMe_2$ double bridges have been synthesized. The analysis of their solid-state structures, determined by single-crystal X-ray measurements, revealed fully planar central six-membered rings. The role of the Si and Ge bridges in the conjugation between the two redox active units has been emphasized upon theoretical calculations, and, accordingly, relies on favorable orbital overlaps between XMe_2 (X = Si, Ge) σ* orbitals and vinylic π* orbitals. The full electron delocalization in the corresponding radical-cation species was clearly assessed upon solution EPR measurements, thus demonstrating sizeable electron communication through the heteroatomic linkers. Finally, conducting charge-transfer compounds, with a pseudo-two-dimensional electronic structure, were prepared by chemical oxidation of $(Me_2Si)_2$(*o*-$DMTTF)_2$ with a 1:1 mixture of TCNQ/$TCNQF_4$, and of $(Me_2Ge)_2$(*o*-$DMTTF)_2$ with TCNQ. Further attempts are under way to prepare new CT complexes and radical-cation salts derived from these new donors, and, also, variation of

the TTF substitution or the bridging heteroatoms is under investigation.

Experimental Section

General: Reactions were carried out under nitrogen, THF was distilled from Na/benzophenone, and dry CH_2Cl_2 was obtained by distillation over P_2O_5. *o*-Me_2TTF was prepared according to a literature method.[21] NMR spectra were recorded on a Bruker Avance DRX 500 spectrometer operating at 500.04 MHz for ^{1}H and 125.75 MHz for ^{13}C. Chemical shifts are expressed in parts per million (ppm) downfield from external TMS. The following abbreviations are used: s, singlet. MALDI-TOF MS spectra were recorded on Bruker Biflex-IIITM apparatus, equipped with a 337 nm N_2 laser. Elemental analyses were performed by the "Service d'Analyse du CNRS" at Gif/Yvette, France.

Synthesis of $(Me_2Si)_2$(*o*-DMTTF)$_2$ (1): Lithium diisopropylamide (8.25 mmol, 5.5 mL of a solution 1.5 M in cyclohexane) was added dropwise to a solution of *o*-DMTTF (0.928 g, 4 mmol) in THF (60 mL) at −78 °C, under magnetic stirring. After a period of 3 h, Me_2SiCl_2 (0.50 mL, 4.2 mmol) was added, then the temperature was allowed to rise slowly overnight up to room temperature. After partial evaporation of THF, addition of a large volume of hexane, filtration, addition of CH_2Cl_2 to the yellow precipitate in order to dissolve the target compound, filtration to eliminate the lithium salts, and rapid chromatographic purification of the filtrate on silica gel with CH_2Cl_2, **1** was recovered as a yellow crystalline solid; yield 0.47 g (40 %). Recrystallization from CH_2Cl_2 afforded yellow, plate-shaped, single crystals suitable for X-ray analysis. ^{1}H NMR ($CDCl_3$): $\delta = 0.39$ (s, 12H; CH_3 of $SiMe_2$), 1.94 ppm (s, 12H; CH_3 of TTF); ^{13}C NMR ($CDCl_3$): $\delta = -0.7$ (s, CH_3 of $SiMe_2$), 13.7 (s, CH_3 of TTF), 108.5–110.9 (s, C=C), 123.0 (s, *C*-Me), 141.1 ppm (s, *C*-$SiMe_2$); MS (MALDI-TOF): *m*/*z*: 576.92 $[M]^+$; elemental analysis calcd (%) for $C_{20}H_{24}S_8Si_2$: C 41.62, H 4.19; found: C 41.12, H 4.14.

Synthesis of $(Me_2Ge)_2$(*o*-DMTTF)$_2$ (2): Lithium diisopropylamide (8.25 mmol, 5.5 mL of a solution 1.5 M in cyclohexane) was added dropwise to a solution of *o*-DMTTF (0.928 g, 4 mmol) in THF (60 mL) at −78 °C, under magnetic stirring. After a period of 3 h, Me_2GeCl_2 (0.50 mL, 4.15 mmol) was added, then the temperature was allowed to rise slowly overnight up to room temperature. After partial evaporation of THF, addition of a large volume of hexane, filtration, addition of CH_2Cl_2 to the yellow precipitate in order to dissolve the target compound, filtration and washing with MeOH to eliminate the lithium salts, washing with Et_2O, and drying, **2** was recovered as a yellow crystalline solid; yield 0.32 g (24 %). Slow evaporation from CH_2Cl_2 afforded yellow plate-shaped single crystals suitable for X-ray analysis. ^{1}H NMR ($CDCl_3$): $\delta = 0.56$ (s, 12H; CH_3 of $GeMe_2$), 1.93 ppm (s, 12H; CH_3 of TTF); ^{13}C NMR ($CDCl_3$): $\delta = -0.2$ (s, CH_3 of $GeMe_2$), 13.7 (s, CH_3 of TTF), 108.4–111.0 (s, C=C), 123.0 (s, *C*-Me), 137.4 ppm (s, *C*-$GeMe_2$); MS (MALDI-TOF): *m*/*z*: 665.74 $[M]^+$; elemental analysis calcd (%) for $C_{20}H_{24}Ge_2S_8$: C 36.06, H 3.63; found: C 35.74, H 3.51.

Synthesis of [1]·1/2[TCNQ]·1/2[$TCNQF_4$]: A solution of **1** (20 mg, 3.47×10^{-2} mmol) in CH_2Cl_2 (5–10 mL) was mixed with a solution of $TCNQF_4$ (4.8 mg, 1.74×10^{-2} mmol) and TCNQ (3.5 mg, 1.74×10^{-2} mmol) in CH_2Cl_2 (10 mL); a sudden change of color into deep green was noted. This resulting mixture was allowed to evaporate slowly, eventually providing brown, plate-shaped crystals of the charge-transfer compound.

Synthesis of [2]·[TCNQ]: A solution of **2** (20 mg, 3×10^{-2} mmol) in CH_2Cl_2 (5–10 mL) was mixed with a solution of TCNQ (6.2 mg, 3×10^{-2} mmol) in CH_2Cl_2 (10 mL); a sudden change of color into deep green was noted. After filtration, the resulting filtrate was allowed to evaporate slowly, providing brown, plate-shaped crystals of the charge-transfer compound.

Table 1. Crystallographic data, details of data collection and structure refinement parameters.

	1	**2**	[**1**]·1/2[TCNQ]·1/2[$TCNQF_4$]	[**2**]·[TCNQ]
formula	$C_{20}H_{24}S_8Si_2$	$C_{20}H_{24}S_8Ge_2$	$C_{32}H_{26}F_2N_4S_8Si_2$	$C_{32}H_{28}Ge_2N_4S_8$
M [g mol^{-1}]	577.05	666.05	817.23	870.24
T [K]	293(2)	293(2)	293(2)	293(2)
crystal system	monoclinic	triclinic	monoclinic	monoclinic
space group	$P2_1/n$	$P\bar{1}$	$C2/m$	$C2/m$
a [Å]	9.2372(10)	9.1950(11)	14.251	14.392(2)
b [Å]	9.7733(9)	14.8873(17)	10.030	10.0812(11)
c [Å]	15.4492(16)	16.0675(19)	14.018	13.981(2)
α [°]	90	73.473(14)	90	90
β [°]	104.764(12)	83.828(14)	113.10	114.995(17)
χ [°]	90	84.338(14)	90	90
V [Å^3]	1348.7(2)	2091.0(4)	1842.9	1838.5(5)
Z	2	3	2	2
ρ_{calcd} [g cm^{-3}]	1.421	1.587	1.473	1.572
μ [mm^{-1}]	0.759	2.763	0.591	2.119
GOF (F^2)	1.003	0.849	1.094	0.897
$R1/wR_2$ [$I>2\sigma(I)$]	0.0395/0.0929	0.0362/0.0778	0.0612/0.1373	0.0339/0.0593
$R1/wR_2$ (all data)	0.0582/0.0986	0.0638/0.0839	0.0945/0.1486	0.0620/0.0653

X-ray structure determinations. Details about data collection and solution refinement are given in Table 1. X-ray diffraction measurements were performed on a Stoe Imaging Plate System for **1**, **2**, and [**2**]·[TCNQ] and on a Bruker Kappa CCD diffractometer for [**1**]·1/2[TCNQ]·1/2-[$TCNQF_4$], both operating with a $Mo_{K\alpha}$ ($\lambda = 0.71073$ Å) X-ray tube with a graphite monochromator. The structures were solved (SHELXS-97) by direct methods and refined (SHELXL-97) by full-matrix least-square procedures on F^2.[22] All non-hydrogen atoms were refined anisotropically, and hydrogen atoms were introduced at calculated positions (riding model), included in structure factor calculations but not refined.

CCDC-632159 (**1**), CCDC-632160 (**2**), CCDC-632161 ([**1**]·1/2[$TCNQF_4$]·1/2[TCNQ]), and CCDC-632162 ([**2**]·[TCNQ]) contain the supplementary crystallographic data for this paper. These data can be obtained free of charge from The Cambridge Crystallographic Data Centre via www.ccdc.cam.ac.uk/data_request/cif.

Electrochemical studies: Cyclic voltammetry measurements were performed by using a three-electrode cell equipped with a platinum millielectrode of 0.126 cm^2 area, an Ag/Ag^+ pseudo-reference and a platinum wire counter electrode. The potential values were then re-adjusted with respect to the saturated calomel electrode (SCE), using the ferrocene as internal reference. The electrolytic media involved a 0.1 mol L^{-1} solution of (n-Bu_4N)PF_6 in CH_2Cl_2. All experiments have been performed at room temperature at 0.1 V s^{-1}. Experiments were carried out with an EGG PAR 273 A potentiostat with positive feedback compensation.

Computational details: Geometry optimizations of **1**, **1**$^{\cdot+}$, **2**, and **2**$^{\cdot+}$ were performed with the Turbomole[23] program package (version 5.8) by using the B-P86 exchange-correlation functional[24] and SV (P)[23] standard basis sets. This basis set had the following contractions: (4s,1p)/[2s,1p] for H, (7s,4p,1d)/[3s,2p,1d] for C, (10s,7p,1d)/[4s,3p,1d] for S, Si and (14s,10p,6d)/[5s,4p,3d] foe Ge. Minima were characterized with harmonic frequency calculations (no imaginary frequencies). The electronic properties and hyperfine coupling constants were obtained with the Gaussian 03 package[25] by running single-point calculations at the optimized geometries and by using the B3LYP functional[26] and the TZVP[27] basis sets (6-311g* for Ge). These basis set had the following contractions: (5s,1p)/[3s,1p] for H, (10s,6p,1d)/[4s,3p,1d] for C, (13s,9p,1d)/[5s,4p,1d] for S, Si and (14s,12p,6d)/[8s,7p,3d] for Ge. Molecular orbitals were represented by using the GaussView program.[28]

Single-crystal conductivity measurements: Electrical resistivity was measured on plate-like shaped crystals of [**1**]·1/2[TCNQ]·1/2[$TCNQF_4$] and [**2**]·[TCNQ]. Four gold contacts were evaporated on the crystals and gold wires were glued with silver paste on those contacts. Resistivity measurements were performed with a four-point method. A low-frequency (<100 Hz) lock-in technique with measuring current $I_{ac}=1$ μA was used for resistance values lower than 20 kOhm, while higher resistances were measured with a dc current ranging from 100 to 1 nA.

Band-structure calculations: The tight-binding band-structure calculations were of the extended Hückel type[29a] with a modified Wolfsberg-Helmholtz formula to calculate the nondiagonal $H_{\mu\nu}$ values.[29b] The basis set consisted of double-ζ Slater-type orbitals for C, Ge, Si, and S and single-ζ Slater-type orbitals for H.

EPR measurements: EPR and ENDOR spectra were recorded on a Bruker ESP 300 spectrometer (X-band) equipped with a variable temperature attachment. Electrochemical oxidations at a controlled potential were performed by using a quartz electrocyclic cell that was present in situ in the EPR cavity. A silver wire electrode was used as a pseudoreference. The working electrode and the counter electrode were platinum. Chemical oxidations were performed under a nitrogen atmosphere in a glove box.

Acknowledgements

Financial support from the French Ministry of Foreign Affairs, Germaine de Staël project, 2006–2007 (PAI 10613RJ) is gratefully acknowledged. This work was also supported by the CNRS (France), the Swiss National Science Foundation (Switzerland) and by MEC-Spain (Project FIS2006-12117-C04-01) and Generalitat de Catalunya (Project 2005-SGR-683).

[1] a) T. Otsubo, Y. Aso, K. Takimiya, *Adv. Mater.* **1996**, *8*, 203; b) M. Iyoda, M. Hasegawa, Y. Miyake, *Chem. Rev.* **2004**, *104*, 5085.
[2] a) J. M. Williams, J. R. Ferraro, R. J. Thorn, K. D. Carlson, U. Geiser, H. H. Wang, A. M. Kini, M.-H. Whangbo, *Organic Superconductors (Including Fullerenes), Synthesis, Structure, Properties and Theory* (Ed.: R. N. Grimes), Prentice-Hall, Englewoods Cliffs, NJ, **1992**; b) T. Ishiguro, K. Yamaji, G. Saito, *Organic Superconductors*, Springer, Heidelberg, **1998**; c) J.-I. Yamada, *TTF Chemistry: Fundamentals and Applications of Tetrathiafulvalene*, Springer, Berlin and Heidelberg, **2004**.
[3] a) M. R. Bryce, *J. Mater. Chem.* **1995**, *5*, 1481; b) M. Fourmigué, C. Mézière, E. Canadell, D. Zitoun, K. Bechgaard, P. Auban-Senzier, *Adv. Mater.* **1999**, *11*, 766; c) C. Mézière, M. Fourmigué, E. Canadell, R. Clérac, K. Bechgaard, P. Auban-Senzier, *Chem. Mater.* **2000**, *12*, 2250.
[4] M. R. Bryce, G. Cooke, A. S. Dhindsa, D. J. Ando, M. B. Hursthouse, *Tetrahedron Lett.* **1992**, *33*, 1783.
[5] a) J. Y. Becker, J. Bernstein, M. Dayan, L. Shahal, *J. Chem. Soc. Chem. Commun.* **1992**, 1048; b) J. D. Martin, E. Canadell, J. Y. Becker, J. Bernstein, *Chem. Mater.* **1993**, *5*, 1199.
[6] a) M. Fourmigué, Y.-S. Huang, *Organometallics* **1993**, *12*, 797; b) F. Gerson, A. Lamprecht, M. Fourmigué, *J. Chem. Soc. Perkin Trans. 2* **1996**, 1409.
[7] S. Perruchas, N. Avarvari, M. Fourmigué, *C. R. Chimie* **2004**, *7*, 895.
[8] a) V. Y. Khodorkovsky, J. Y. Becker, J. Bernstein, *Synth. Met.* **1993**, *56*, 1931; b) E. Aqad, J. Y. Becker, J. Bernstein, A. Ellern, V. Khodorkovsky, L. Shapiro, *J. Chem. Soc. Chem. Commun.* **1994**, 2775.
[9] a) C. Wang, A. Ellern, J. Y. Becker, J. Bernstein, *Tetrahedron Lett.* **1994**, *35*, 8489; b) C. Wang, A. Ellern, V. Khodorkovsky, J. Y. Becker, J. Bernstein, *J. Chem. Soc. Chem. Commun.* **1994**, 2115.
[10] N. Avarvari, M. Fourmigué, *Chem. Commun.* **2004**, 2794.
[11] M. Ashizawa, H. M. Yamamoto, A. Nakao, R. Kato, *Tetrahedron Lett.* **2006**, *47*, 8937.
[12] a) J. Kreisz, R. U. Kirss, W. M. Reiff, *Inorg. Chem.* **1994**, *33*, 1562; b) D. L. Zechel, D. A. Foucher, J. A. Pudelski, G. P. A. Yap, A. L. Rheingold, I. Manners, *J. Chem. Soc. Dalton Trans.* **1995**, 1893; c) H. Atzkern, P. Bergerat, H. Beruda, M. Fritz, J. Hiermeier, P. Hudeczek, O. Kahn, F. H. Köhler, M. Paul, B. Weber, *J. Am. Chem. Soc.* **1995**, *117*, 997; d) F. H. Köhler, A. Schell, B. Weber, *J. Organomet. Chem.* **1999**, *575*, 33; e) M. Herker, F. H. Köhler, M. Schwaiger, B. Weber, *J. Organomet. Chem.* **2002**, *658*, 266.
[13] Details are provided in the Supporting Information.
[14] U. Siemeling, P. Jutzi, B. Neumann, H.-G. Stammler, *Organometallics* **1992**, *11*, 1328.
[15] a) S. Yamaguchi, K. Tamao, *Bull. Chem. Soc. Jpn.* **1996**, *69*, 2327; b) S. Yamaguchi, C. Xu, H. Yamada, A. Wakamiya, *J. Organomet. Chem.* **2005**, *690*, 5365; c) S. Yamaguchi, C. Xu, K. Tamao, *J. Am. Chem. Soc.* **2003**, *125*, 13662.
[16] Nine of the thirteen expected lines are observed in the spectrum. As shown in Supporting Information, the intensity distribution is in good accordance with the simulated spectrum.
[17] C. Gouverd, F. Biaso, L. Cataldo, T. Berclaz, M. Geoffroy, E. Levillain, N. Avarvari, M. Fourmigué, F. X. Sauvage, C. Wartelle, *Phys. Chem. Chem. Phys.* **2005**, *7*, 85.
[18] a) M. B. Robin, P. Day, *Adv. Inorg. Chem. Radiochem.* **1967**, *10*, 247; b) B. B. Brunschweig, C. Creutz, N. Sutin, *Chem. Soc. Rev.* **2002**, *31*, 168.
[19] T. J. Kistenmacher, T. J. Emge, A. N. Bloch, D. O. Cowan, *Acta Crystallogr. Sect. B* **1982**, *38*, 1193.
[20] A. Bondi, *J. Phys. Chem.* **1964**, *68*, 441.
[21] F. Gerson, A. Lamprecht, M. Fourmigué, *J. Chem. Soc. Perkin Trans. 2* **1996**, 1409.
[22] G. M. Sheldrick, *Programs for the Refinement of Crystal Structures*, University of Göttingen, Göttingen (Germany), **1996**.
[23] R. Ahlrichs, M. Bär, M. Häser, H. Horn, C. Kölmel, *Chem. Phys. Lett.* **1989**, *162*, 165.
[24] R. Ahlrichs, F. Furche, S. Grimme, *Chem. Phys. Lett.* **2000**, *325*, 317.
[25] Gaussian 03, Revision B.03, M. J. Frisch, G. W. Trucks, H. B. Schlegel, G. E. Scuseria, M. A. Robb, J. R. Cheeseman, J. A. Montgomery, Jr., T. Vreven, K. N. Kudin, J. C. Burant, J. M. Millam, S. S. Iyengar, J. Tomasi, V. Barone, B. Mennucci, M. Cossi, G. Scalmani, N. Rega, G. A. Petersson, H. Nakatsuji, M. Hada, M. Ehara, K. Toyota, R. Fukuda, J. Hasegawa, M. Ishida, T. Nakajima, Y. Honda, O. Kitao, H. Nakai, M. Klene, X. Li, J. E. Knox, H. P. Hratchian, J. B. Cross, V. Bakken, C. Adamo, J. Jaramillo, R. Gomperts, R. E. Stratmann, O. Yazyev, A. J. Austin, R. Cammi, C. Pomelli, J. W. Ochterski, P. Y. Ayala, K. Morokuma, G. A. Voth, P. Salvador, J. J. Dannenberg, V. G. Zakrzewski, S. Dapprich, A. D. Daniels, M. C. Strain, O. Farkas, D. K. Malick, A. D. Rabuck, K. Raghavachari, J. B. Foresman, J. V. Ortiz, Q. Cui, A. G. Baboul, S. Clifford, J. Cioslowski, B. B. Stefanov, G. Liu, A. Liashenko, P. Piskorz, I. Komaromi, R. L. Martin, D. J. Fox, T. Keith, M. A. Al-Laham, C. Y. Peng, A. Nanayakkara, M. Challacombe, P. M. W. Gill, B. Johnson, W. Chen, M. W. Wong, C. Gonzalez, J. A. Pople, Gaussian, Inc., Wallingford CT, **2004**.
[26] A. D. Becke, *J. Chem. Phys.* **1993**, *98*, 5648.
[27] This basis set was obtained from the Extensible Computational Chemistry Environment Basis set Database, Version 02/25/04 as developed and distributed by the Molecular Science Computing Facility, Environmental and Molecular Sciences Laboratory, Richland, Washington 99352 (USA); N. Godbout, D. R. Salahub, J. Andzelm, E. Wimmer, *Can. J. Chem.* **1992**, *70*, 560.
[28] GaussView 3.0, Gaussian, Inc., Pittsburgh, PA.
[29] a) M.-H. Whangbo, R. Hoffmann, *J. Am. Chem. Soc.* **1978**, *100*, 6093; b) J. H. Ammeter, H.-B. Bürgi, J. Thibeault, R. Hoffmann, *J. Am. Chem. Soc.* **1978**, *100*, 3686.

Received: February 9, 2007
Published online: April 17, 2007

